Chemoattractive Activity of Sonic Hedgehog in the Adult Subventricular Zone Modulates the Number of Neural Precursors Reaching the Olfactory Bulb

Elodie Angot, Karine Loulier, Kim T. Nguyen-Ba-Charvet, Alain-Pierre Gadeau, Martial Ruat, Elisabeth Traiffort

STEM CELLS®

THE STEM CELL NICHE

Chemoattractive Activity of Sonic Hedgehog in the Adult Subventricular Zone Modulates the Number of Neural Precursors Reaching the Olfactory Bulb

ELODIE ANGOT,[a] KARINE LOULIER,[a] KIM T. NGUYEN-BA-CHARVET,[b] ALAIN-PIERRE GADEAU,[c] MARTIAL RUAT,[a] ELISABETH TRAIFFORT[a]

[a]Signal Transduction and Developmental Neuropharmacology Team, Laboratoire de Neurobiologie Cellulaire et Moleculaire, Institut de Neurobiologie Alfred Fessard, Centre National de la Recherche Scientifique, Gif-sur-Yvette, France; [b]Université Pierre et Marie Curie, Unité Mixte de Recherche 7102, Paris, France; [c]Institut National de la Santé et de la Recherche Médicale, Unité 828, Pessac, France

Key Words. Hedgehog • Adult stem cell • Subventricular zone • Cell migration

ABSTRACT

The adult subventricular zone (SVZ) supports neural stem cell self-renewal and differentiation and continually gives rise to new neurons throughout adult life. The mechanisms orienting the migration of neuroblasts from the SVZ to the olfactory bulb (OB) via the rostral migratory stream (RMS) have been extensively studied, but factors controlling neuroblast exit from the SVZ remain poorly explored. The morphogen Sonic Hedgehog (Shh) displays proliferative and survival activities toward neural stem cells and is an axonal chemoattractant implicated in guidance of commissural axons during development. We identify here the presence of Shh protein in SVZ extracts and in the cerebrospinal fluid of adult mice, and we demonstrate that migrating neuroblasts in the SVZ and RMS express the Shh receptor Patched. We show that Shh displays a chemoattractive activity in vitro on SVZ-derived neuronal progenitors, an effect blocked by Cur61414, a Smoothened antagonist. Interestingly, Shh-expressing cells grafted above the RMS of adult mice exert a chemoattractive activity on migrating neuroblasts in vivo, thus inducing their accumulation and deviation from their normal migratory pathway. Furthermore, the adenoviral transfer of Shh into the lateral ventricle or the blocking of Shh present in the SVZ of adult mice using its physiological antagonist Hedgehog interacting protein or neutralizing Shh antibodies provides in vivo evidence that Shh can retain SVZ-derived neuroblasts. The ability to modulate the number of neuroblasts leaving the SVZ and reaching the OB through the chemoattractive activity of Shh suggests a novel degree of plasticity in cell migration of this adult stem cell niche. STEM CELLS *2008;26:2311–2320*

Disclosure of potential conflicts of interest is found at the end of this article.

INTRODUCTION

The subventricular zone (SVZ) of the lateral ventricles (LV) constitutes a major site of neurogenesis, providing new neurons to the olfactory bulb (OB) throughout life [1]. This niche contains quiescent adult neural stem cells that can generate transit-amplifying cells, the primary precursors of neuroblasts [2, 3]. Before they become interneurons functionally integrated into the OB, neuroblasts migrate in chains along the rostral migratory stream (RMS), a restricted area limited by glial cell tubes. Polarized epithelial cells bordering the LV contribute to their initial orientation [4], and several factors are involved in their migration [3] by maintaining a permissive environment, participating in their motility, promoting the formation of cell chains, maintaining the integrity of glial tubes [5], or acting as chemorepellents. In the OB, other factors behave as signals leading the neuroblasts to detach from the chains or acting as chemoattractants for these cells. However, factors that may balance the local repulsive activity allowing neuroblasts to leave the SVZ remain to be investigated.

The involvement of Hedgehog (Hh) morphogens has been reported in migratory processes in several embryonic tissues [6, 7] or in the navigation of axons. For instance, Sonic Hedgehog (Shh), expressed in the floor plate, behaves first as an attractive signal for commissural axons [8, 9] and then as a repulsive factor when the axons have crossed the floor plate and turned rostrally [10]. Shh mediates its actions through the 12-pass transmembrane protein Patched (Ptc), the G protein-coupled receptor Smoothened (Smo), and the type I transmembrane protein Hedgehog interacting protein (Hip), characterized as the natural negative regulator of Hh morphogens. The intracellular

Author contributions: E.A.: collection and/or assembly of data, data analysis and interpretation, manuscript writing; K.L. and K.T.N.-B.-C.: collection and/or assembly of data, data analysis and interpretation; A.-P.G.: provision of study material or patients; M.R.: conception and design, financial support, data analysis and interpretation, manuscript writing; E.T.: conception and design, collection and/or assembly of data, data analysis and interpretation, manuscript writing.

Correspondence: Martial Ruat, Ph.D., Centre National de la Recherche Scientifique, Institut de Neurobiologie Alfred Fessard-IFR 2118, UPR9040, Laboratoire de Neurobiologie Cellulaire et Moleculaire, Signal Transduction and Developmental Neuropharmacology team, Batiment 33, 1 avenue de la Terrasse, F-91198, Gif-sur-Yvette, France. Telephone: 33169823641; Fax: 33169823639; e-mail: ruat@nbcm.cnrs-gif.fr Received March 26, 2008; accepted for publication June 29, 2008; first published online in STEM CELLS *EXPRESS* July 10, 2008. 1066-5099/2008/$30.00/0 doi: 10.1634/stemcells.2008-0297

cascade triggered by the pathway activation involves the transcription factors Gli1–3 [11–13]. In the adult rodent brain, Shh signaling is still present and active [14–17]. Shh is involved in the control of electrophysiological properties of mature neurons [18, 19], but is also a mitogen for adult progenitors residing in the dentate gyrus [20] and in the cerebral cortex [21]. Conditional Smo removal led to the proposal that Hh pathway is required for the maintenance of adult neural stem cells in the SVZ [22–24]. There, Shh-responding cells were characterized as being the quiescent stem- and transit-amplifying cells on the basis of the expression of the Shh-associated transcription factor Gli1 [25]. However, Shh does not increase cell proliferation in the SVZ after its acute delivery into the LV of adult mice [21] and is unable to support neurosphere expansion in the absence of epidermal growth factor [26].

Here, we have investigated the potential implication of Shh in other processes linked to forebrain neurogenesis. We identify the presence of Shh in SVZ extracts and in the cerebrospinal fluid (CSF) of adult mice and demonstrate migrating neuroblasts in the SVZ and RMS express the Shh receptor Ptc. Combining in vivo gain- and loss-of-function experiments and ex vivo approaches to modulate the pathway activity, we show that Shh present in the SVZ displays a chemoattractive activity on SVZ-derived neuroblasts and is thus able to modulate the number of these cells integrating into the OB.

Materials and Methods

Animals

Male 8-week-old OF1 (Charles River Laboratories, Wilmington, MA, http://www.criver.com) and heterozygous $Ptc^{+/-}$ *LacZ* mice [27] were used.

In Situ Hybridization

Experiments using Ptc-, Smo-, and Hip-specific probes were performed as previously described [15, 16].

Western Blot Analysis

Expression of the active N-terminal fragment of Shh protein (ShhN) was investigated on mouse tissue preparations of whole brain, SVZ, and choroid plexuses (ChPl) obtained after centrifugation of tissue homogenates (9,000*g* for 20 minutes). For the SVZ, 0.4-mm-thick coronal slices were performed through freshly dissected brains to obtain a 0.5-mm-wide, 1.5-mm-long strip of the wall of the anterior LV and medial part of the striatum containing the SVZ. The CSF was collected from the cisterna magna in deeply anesthetized mice (described below). The samples were centrifuged at 200*g* for 15 minutes before gel loading. The pellet fractions for SVZ, ChPl (40 μg of proteins), the homogenate for the whole brain (30 μg), and the supernatant for CSF (20 μl) were analyzed using the ShhN-specific antiserum 167Ab [17]. The effective quantity of loaded protein was determined by probing the blots with a 1:500 dilution of the mouse monoclonal IgG2a α-actin antibody (AC-40; Sigma-Aldrich, St. Louis, http://www.sigmaaldrich.com). For ShhN expression in the homogenates and culture supernatants of transfected COS cell aggregates, aliquots of COS(Shh) and COS(mock) cells and their respective culture media were harvested at the end of the coculture experiment. The culture media were acetone-precipitated before loading. Hip expression was investigated on homogenates and culture media from CHO-K1 cells (1.5×10^6/3 ml) harvested 24 hours after infection with increasing concentrations of the adenoviral vector expressing Hip. Analysis of the secretion of 5E1 and 9E10 was performed on an aliquot of the culture medium of hybridoma cells cultured at the same density (0.2×10^6 cells per plate) using a biotin-conjugated anti-mouse IgG (Vector Laboratories, Burlingame, CA, http://www.vectorlabs.com).

Adenovirus Production

Adenoviral vectors (Ad) were generated by the Genethon Viral Production Network (Genopôle, Evry, France, http://www.genopole.org): AdhuShh-eGFP and Ad-eGFP have been described [21]; pAd/CMVmHip:IRES:eGFP corresponds to the Ad containing mouse Hip (mHip) cDNA (from Dr. A.P. McMahon) under the control of the constitutive cytomegalovirus promoter, placed in tandem sequence with enhanced green fluorescent protein (eGFP) under the control of an internal ribosomal entry site. Replication-defective recombinant type 5 adenoviruses (AdmHip-eGFP) were obtained.

Injections of Adenoviral Vectors and Bromodeoxyuridine

Groups of OF1 mice were deeply anesthetized with a ketamine (0.1 mg/g; Merial, Duluth, GA, http://www.merial.com)/xylazine (0.01 mg/g; Bayer, Leverkusen, Germany, http://www.bayer.com) mixture and stereotaxically injected into the right LV (anteroposterior, +0.2 mm; lateral, +0.8 mm; dorsoventral, −2.5 mm) with 0.75×10^8 (AdhuShh-eGFP, Ad-eGFP) or 1.5×10^8 (AdmHip-eGFP, Ad-eGFP) plaque-forming units in a volume of 3 μl. Mice received a once-daily intraperitoneal (i.p.) injection of bromodeoxyuridine (BrdU; Sigma-Aldrich) between day 4 and day 18, before being sacrificed at day 26 ($n = 5–6$ for each group). All procedures were carried out in accordance with the European Community Council Directive (86/806/EEC) for the care and use of laboratory animals.

Tissue Processing and Immunostaining

Frontal brain sections (16 μm) were processed and immunostained with primary antibodies against β-galactosidase (βgal; 1:1,000; MP Biomedicals, Irvine CA, http://www.mpbio.com), Hip (1:1,000) [15], Shh (1:300) [21], BrdU (1:200), glial fibrillary acidic protein (GFAP) (1:500), neuronal nuclei (NeuN) (1:1,000), NG2 proteoglycan (1:500), and poly-sialated neural cell adhesion molecule (PSA-NCAM) (1:400), as described [21]. The secondary antibodies were as follows: biotinylated goat anti-rat IgG (1:200; Vector Laboratories), goat anti-rabbit IgG (1:200; Sigma-Aldrich), fluorescein isothiocyanate (FITC)- or tetramethylrhodamine B isothiocyanate-conjugated goat anti-rat IgG (1:200; Jackson Immunoresearch Laboratories, West Grove, PA, http://www.jacksonimmuno.com), FITC-conjugated anti-mouse IgG and IgM (1:200; Sigma-Aldrich), anti-mouse and anti-rabbit IgG Alexa Fluor 546 (1:1,000; Invitrogen, Carlsbad, CA, http://www.invitrogen.com), and anti-rabbit IgG Cy5 (1:500; Jackson Immunoresearch Laboratories). Immunofluorescent signals were detected by a conventional epifluorescence microscope (DMRXA2; Leica, Heerbrugg, Switzerland, http://www.leica.com) equipped with a camera (Photometrics CoolSnap; Roper Scientific, Tucson, AZ, http://www.roperscientific.com). Terminal deoxynucleotidyl transferase dUTP nick-end labeling (TUNEL) experiments (Apoptag^R Peroxidase In situ Apoptosis Detection Kit; Millipore, Billerica, MA, http://www.millipore.com) were performed using the supplier's protocol.

Counting and Statistical Analysis

Visilog 6.4 Xpert software (Noesis, Saint-Aubin, France, http://noesisvision.com), for which specific applications were developed, was used for counting cells labeled with BrdU alone or together with a second marker (GFAP, NeuN, NG2). Labeled nuclei or cells were counted within the entire SVZ (between bregma levels −0.1 and +1.2) and in the granular or glomerular layers of the whole or ventral third (for double histofluorescence experiments) of the OB. The region of interest was defined by the experimenter, and systematic errors were restricted by an automatic filter excluding staining, which did not display the criteria initially defined for the morphology, the size and the intensity of the signal. Estimation of the total number of $BrdU^+$ cells in the whole SVZ-RMS-OB system was performed as previously described [28], using comparable levels in each group of animals. The areas of the SVZ (between −0.10 and 1.18 mm from the bregma), RMS (between 1.42 and 4.28 mm from the bregma), and granule cell layer of the OB (between 2.58 and 4.28 mm from the bregma) were measured in

coronal 16-μm-thick serial sections at 256-μm (SVZ, OB) or 512-μm (RMS) intervals using Visilog 6.4 Xpert software. The volume of each of these brain structures was approximated with the equation $\Sigma(_{i\ =\ 0\ \text{to}\ n})A_i\ d$, where A equals the area of the ith section, d is the distance between sections, and n is the total number of measured sections. The total number (T) of BrdU-immunostained nuclei in SVZ-RMS-OB system was estimated using the following formula: $T = (N_{SVZ} \times V_{SVZ})/t + (N_{RMS} \times V_{RMS})/t + (N_{OB} \times V_{OB})/t$, where N is the number of $BrdU^+$ nuclei per unit area in each brain structure (SVZ, RMS, or OB), V is the volume of each brain structure, and t is the section thickness. Statistical analysis was performed using the unpaired bilateral Student's t test. Statistical significance was considered for $p < .05$.

Collagen Coculture Assays

The protocol was adapted from Nguyen-Ba-Charvet et al. [29]. SVZ explants were excised from brains of P6 OF1 mice, and aggregates of COS7 cells were obtained by the hanging drop method following their transient transfection the day before with DNA (1 μg) of pRK5 expressing human full-length Shh (pRK5-huShh) or nonrecombinant vector (pRK5) using Fugene-6 (Roche Diagnostics, Basel, Switzerland, http://www.roche-applied-science.com). Cur61414 (5 μM in H_2O) was added into both the collagen gel and culture medium. Thirty-six hours after the beginning of the coculture, samples were fixed in 4% paraformaldehyde (1 hour), carefully removed from culture dishes, permeabilized (0.1% Triton X-100), and blocked (1% normal goat serum; Invitrogen) overnight. Incubation with mouse neuron-specific class III beta-tubulin (Tuj1) antibody (1:2,000; Covance, Princeton, NJ, http://www.covance.com) was carried out overnight at 4°C, before extensive washes and incubation with Alexa Fluor 546 goat anti-mouse IgG (1:1,000). Images were obtained with the DMRXA2 microscope. Quantification of migrating cells and of their migration distance were carried out on fluorescence images with Visilog 6.4 Xpert software (Noesis). The field was divided into four orthogonal quadrants, and the number of 4,6-diamidino-2-phenylindole$^+$/Tuj1$^+$ migratory neuroblasts was counted in the area excluding the explant itself, in the proximal (P) and distal (D) quadrants with respect to the cell aggregate. For each explant, the P/D ratio was calculated and used as a chemoattraction index. For the migration distances, the barycenter of each explant was determined before measuring the distance covered by each cell from the explant edge.

Grafting Experiments

The stable QT6 cell line expressing the full-length chicken Shh (QT6-Shh) and its control cell line (QT6) (from D. Duprez, Université Pierre et Marie Curie, Paris) [17] were maintained in Dulbecco's modified Eagle's medium supplemented with fetal bovine serum (FBS; 8%), chick serum (2%), and geniticin (800 mg/l) (all from Invitrogen). The hybridoma cell lines 5E1 and 9E10 (Developmental Studies Hybridoma Bank, Iowa City, IA, http://www.uiowa.edu/~dshbwww; gift from E.T. Stoeckli) secreting the specific Shh antibody and a specific isotype, respectively, were maintained in Iscove's modified Dulbecco's medium (Invitrogen) supplemented with FBS (20%) and gentamicin (50 mg/l; Invitrogen). On the day of transplantation, cells were labeled with the PKH26 red fluorescent cell linker kit (Sigma-Aldrich) according to the supplier's protocol and immediately used for transplantation. Adult male OF1 mice (30–35 g; $n = 6$ for each group) were deeply anesthetized. Cells (2×10^5) were stereotaxically injected under a volume of 1 μl (QT6, QT6-Shh) or 2 μl (5E1, 9E10) next to the vertical limb of RMS (QT6, QT6-Shh; anteroposterior, +2.2 mm; mediolateral, +1.0 mm; dorsoventral, −3.0 mm) or into the right LV (5E1, 9E10; anteroposterior, +0.2 mm; mediolateral, +0.8 mm; dorsoventral, −2.5 mm). Mice either were sacrificed 4 days later (QT6, QT6-Shh) or received a daily i.p. injection of BrdU (50 mg/kg) between day 1 and day 11 before being sacrificed at day 20 (5E1, 9E10). In the experiments using the grafts of QT6 cells, the counting of cells deviating from their normal way through the RMS were carried out by a blind experimenter, who drew a line bordering the most external part of the "regular" RMS, which means the RMS that does not face the cell graft. All PSA-NCAM$^+$ cells located between this line and the grafted QT6-Shh cells were counted over an RMS length of 800 μm. Determination of the total number of $BrdU^+$ cells in the RMS was performed on sagittal sections containing the greatest extent of the RMS located at comparable levels in all QT6-Shh- and control QT6-treated animals.

RESULTS

Shh Protein and Ptc-Smo Transcripts Are Expressed in the Adult SVZ-RMS System

Western blot analysis of freshly microdissected strips of the striatum containing LV wall including the SVZ of adult mice showed that ShhN was present. These data are in agreement with previous observations reporting the expression of Shh transcripts in the lateral wall of the LV of adult mice [26]. We also found the presence of ShhN in the CSF of these animals but not in the ChPl (Fig. 1A). Therefore, ShhN produced in the wall of the LV may act locally on SVZ cells or at a distance after its diffusion through the CSF. To investigate whether SVZ and RMS contain Shh-responding cells, we analyzed the expression of Ptc, Smo, and Hip mRNAs by in situ hybridization. Consecutive sections of adult mouse brain showed Ptc (Fig. 1B) and Smo (Fig. 1D) expression in the SVZ lining the LV and in the entire RMS from the most caudal regions (close to the SVZ) to the most rostral ones (close to the OB), whereas Hip mRNA was identified in a few "en passant" small-sized cells (data not shown). No labeling was detected when the corresponding Ptc (Fig. 1C) or Smo (Fig. 1E) sense riboprobes were used. In addition, as positive control, we detected Ptc transcripts in the granular and Purkinje cell layers of the cerebellar cortex, as previously described (Fig. 1N) [16]. Adult $Ptc^{+/-}$ mice with a *lacZ* reporter gene inserted in the deleted allele [27] showed a clear βgal signal in both the SVZ and the RMS (Fig. 1H, 1L). As the expression pattern of Ptc in the SVZ/RMS was compatible with that of PSA-NCAM, a marker of migrating neuroblasts [30], we then analyzed the coexpression of Ptc with this marker. βgal^+ cells have been detected coexpressing PSA-NCAM in both the SVZ (Fig. 1F–1I) and the RMS (Fig. 1J–1M). Interestingly, in addition to double-labeled βgal^+/PSA-NCAM$^+$ cells, βgal^+/PSA-NCAM$^-$ cells were also found in the SVZ, in agreement with the previously reported expression of Ptc in quiescent stem- and transit-amplifying cells [26]. As a control, in the same experiment, βgal^+ cells were detected in the granular and Purkinje cell layers of the cerebellar cortex (Fig. 1O–1Q), consistent with Ptc transcript localization in this area (Fig. 1N) [27]. Together, these data demonstrate that migrating neuroblasts in the SVZ-RMS system are Shh-responding cells and are compatible with a direct effect of Shh present within the SVZ on the control of the properties of these cells.

Blocking Shh Pathway by Hip Overexpression Modifies the Number of BrdU$^+$ Cells in Both the SVZ and OB In Vivo

To investigate the effect induced by the blocking of Shh activity in the SVZ in vivo on the migrating neuroblasts, we developed an adenoviral vector (AdmHip-eGFP) bearing the gene encoding Hip, the natural negative regulator of the Hh morphogen pathway. CHO-K1 cells infected by AdmHip-eGFP produced Hip-soluble forms that can block Shh-induced differentiation of the mesenchymal C3H10T1/2 cell line [15] (supplemental online Fig. 1A, 1B; data not shown). Adult mice were injected with AdmHip-eGFP or the corresponding control (Ad-eGFP) into the right LV and received a daily i.p. injection of BrdU between day 4 and day 18 to label slowly and quickly dividing cells. The animals were analyzed on day 26 to allow cells that had incorporated BrdU to reach the OB (Fig. 2A). Then, the brains were processed for Hip and BrdU

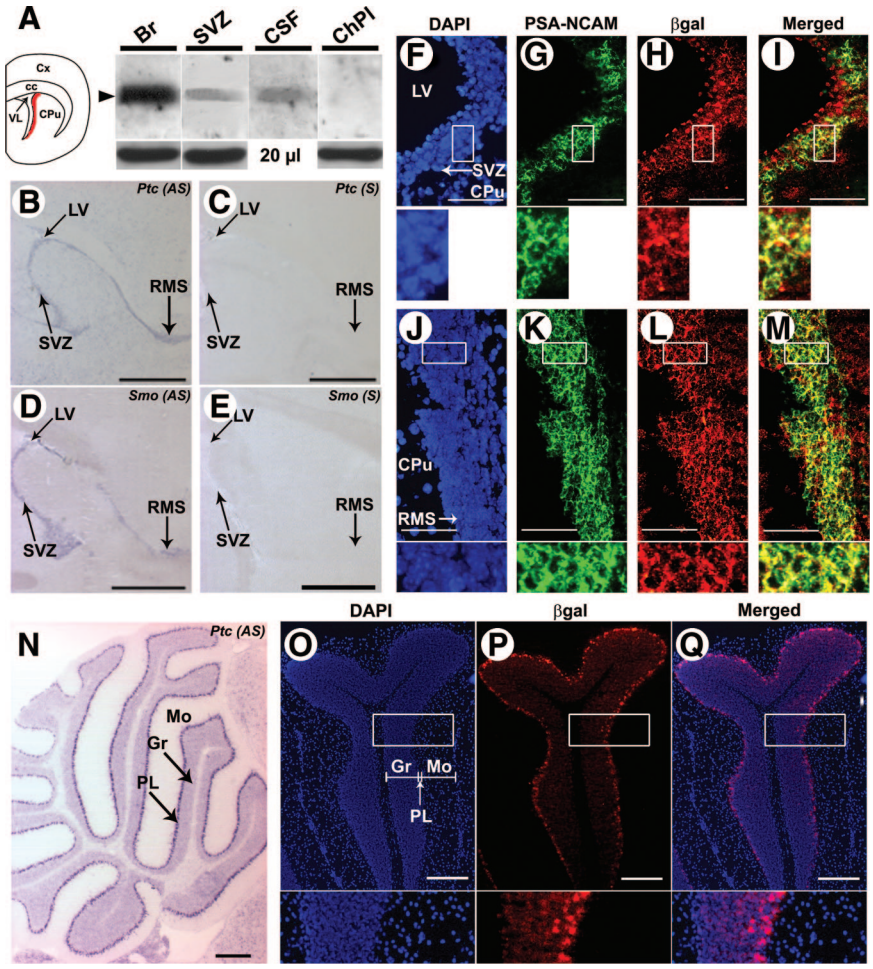

Figure 1. Presence of the Sonic Hedgehog (Shh) protein and its receptors Ptc-Smo in the SVZ-RMS system of adult mouse brain. **(A):** Western blot analysis showing ShhN protein expression as a 22-kDa signal (arrowhead) in extracts of SVZ strips (red on the scheme of a frontal brain section), in the CSF (20 μl) but not in ChPl. Br is shown as a positive control. Protein loading was analyzed with anti-actin (bottom panel). **(B–E):** Sagittal sections showing Ptc **(B)** and Smo **(D)** transcripts in the SVZ and RMS. No labeling was detected when the corresponding Ptc **(C)** and Smo **(E)** sense probes were used. **(F–M):** Sagittal **(F–I)** and coronal **(J–M)** slices from adult $Ptc^{+/-}$ *LacZ* mice double-labeled for PSA-NCAM (green in **[G, K]**) and βgal (red in **[H, L]**) in the SVZ **(F–I)** and RMS **(J–M)**. The overlays show βgal^{+}/$PSA\text{-}NCAM^{+}$ cells (yellow) in both the SVZ **(I)** and RMS **(M)**. Magnifications of the boxed areas are shown below each panel. Nuclei are in blue (DAPI in **[F, J]**). **(N–Q):** Positive controls of in situ hybridization and βgal labeling showing the expected Ptc expression profile in the cerebellum. **(N):** A sagittal section of adult mouse brain was hybridized using the specific Ptc antisense riboprobe. The signal was detected in the Gr and PL. **(O–Q):** βgal expression (red in **[P]**) was clearly detected in the PL and to a lesser extent in the Gr, visualized by the DAPI fluorescence **(O)** on a sagittal section from heterozygous $Ptc^{+/-}$ *LacZ* mice. No βgal staining was detected in the Mo. The merged picture is presented in **(Q)**. A higher magnification of the boxed areas in **(O–Q)** is shown below each panel. Scale bars = 1 mm **(B–E)**, 100 μm **(F–M)**, 800 μm **(N)**, and 400 μm **(O–Q)**. Abbreviations: AS, antisense; βgal, β-galactosidase; Br, whole brain; cc, corpus callosum; ChPl, choroid plexuses; CPu, caudate putamen; CSF, cerebrospinal fluid; Cx, cortex; DAPI, 4,6-diamidino-2-phenylindole; Gr, granular cell layer; LV, lateral ventricle; Mo, molecular layer; PL, Purkinje cell layer; PSA-NCAM, poly-sialated neural cell adhesion molecule; Ptc, Patched; RMS, rostral migratory stream; S, sense; Smo, Smoothened; SVZ, subventricular zone.

immunoreactivity. A robust Hip expression was observed in infected cells bordering the walls from the LV to the olfactory ventricles and was detected over several cell diameters inside the parenchyma (supplemental online Fig. 1C–1E; data not shown). Thus, in these brain areas, ShhN can likely interact with Hip protein. $BrdU^{+}$ nuclei were observed in the SVZ and the RMS and were found scattered throughout the granule cell layer of the OB, the expected final location of newly generated cells. Upon AdmHip-eGFP treatment, the mean density of $BrdU^{+}$ nuclei was significantly decreased by 17% ($p < .01$) in the SVZ and increased by 119% ($p < .001$) in the granular layer (Fig. 2B–2E, 2H, 2I). In the more external glomerular layer where newly generated interneurons derived less from the SVZ and more from the RMS itself [31], the mean density of $BrdU^{+}$ nuclei was not significantly modified (Fig. 2F, 2G, 2J), suggesting that the Hip treatment does not affect this precursor population. Thus, the inhibition of Shh activity in the SVZ by its natural negative regulator leads to a decrease in the SVZ and an increase in $BrdU^{+}$ cell number in the granular cell layer of the OB. To investigate the potential existence of a proliferation/survival effect of Hip on neural cell precursors, we estimated the total number of $BrdU^{+}$ cells in the whole SVZ-RMS-OB system for each group of animals as described in Materials and Methods. We found 100,613 $\pm$ 10,840 $BrdU^{+}$ nuclei in the SVZ-RMS-OB system of AdmHip-eGFP-treated mice versus 91,760 $\pm$ 10,211 in Ad-eGFP-treated mice ($p > .05$), indicating that Hip does not likely regulate proliferation/survival of adult neural precursors (Fig. 2K). In agreement with this result, determination of cell apoptosis in the SVZ using TUNEL analysis did not allow the detection of any significant difference between AdmHip-eGFP- and Ad-eGFP-treated mice (supplemental online Fig. 2). Together, these data clearly suggest a role of Shh pathway in the modulation of the number of precursors in both the SVZ and the OB.

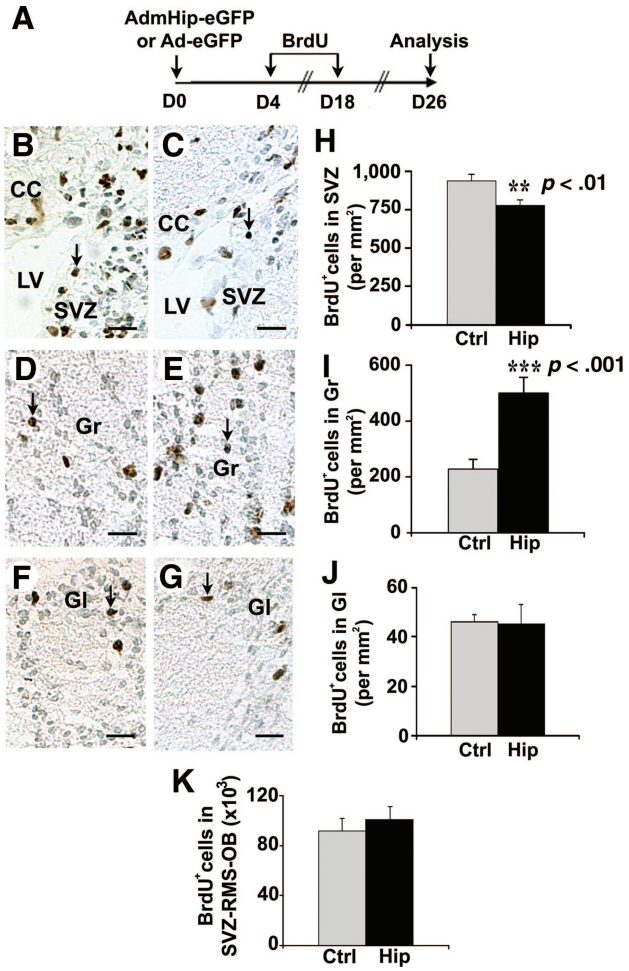

Figure 2. Blocking Sonic Hedgehog by Hip modifies the number of BrdU$^+$ cells in the SVZ and the OB in vivo. **(A):** Scheme of experimental protocol. **(B–G):** BrdU$^+$ nuclei are visualized in brown (a few are indicated by an arrow) on coronal brain sections at the level of the SVZ of the LV **(B, C)**, the Gr **(D, E)**, and the Gl **(F, G)** of the OB in Ad-eGFP-treated **(B, D, F)** and AdmHip-eGFP-treated **(C, E, G)** mice. **(H–J):** In AdmHip-eGFP (Hip)- compared with Ad-eGFP (Ctrl)-treated mice, the number of BrdU$^+$ nuclei was decreased in the SVZ (775 ± 39 [total counted cells, n = 1,961] and 936 ± 43 cells per mm^2 [n = 3,206], respectively) **(H)**, increased in the Gr (500 ± 55 [n = 6,532] and 229 ± 35 cells per mm^2 [n = 2,303], respectively) **(I)**, and not significantly different in the Gl of the OB (45 ± 8 [n = 526] and 46 ± 3 cells per mm^2 [n = 1,481], respectively; $p > .05$) **(J)**. **(K):** The total number of BrdU$^+$ cells in the whole SVZ-RMS-OB system was not significantly different in Hip- compared with Ctrl-treated mice (100,613 ± 10,840 and 91,760 ± 10,211 cells, respectively; $p > .05$). The volumes (mm^3) of the structures determined for Hip- and Ctrl-treated mice were as follows: 0.104 ± 0.008 and 0.124 ± 0.006 (SVZ); 0.216 ± 0.032 and 0.230 ± 0.021 (RMS); and 3.110 ± 0.267 and 3.149 ± 0.077 (OB), respectively. Data are the means ± SEM from four or five mice per group. **, $p < .01$; ***, $p < .001$. Scale bars = 25 μm. Abbreviations: BrdU, bromodeoxyuridine; CC, corpus callosum; Ctrl, control; D, day; eGFP, enhanced green fluorescent protein; Gl, glomerular layer; Gr, granular cell layer; Hip, Hedgehog interacting protein; LV, lateral ventricle; OB, olfactory bulb; RMS, rostral migratory stream; SVZ, subventricular zone.

Hip Does Not Reorient the Phenotype or Influence the Survival of Cells Reaching the OB

To investigate whether Hip overexpression is able to influence the phenotype of cells reaching the OB, we first used double immunohistofluorescence with anti-BrdU antibodies and specific cell markers for astrocytes (GFAP) or mature neurons (NeuN). The

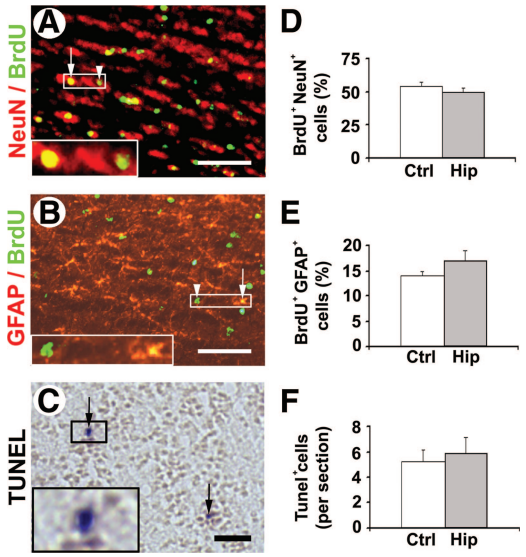

Figure 3. The adenovirus-mediated transfer of Hip into the lateral ventricle does not influence the phenotype of cells reaching the olfactory bulb (OB). **(A–C):** Double immunohistofluorescence for BrdU (green in **[A, B]**) and markers of mature neurons (NeuN; red in **[A]**) or astrocytes (GFAP; red in **[B]**) and visualization of TUNEL$^+$ nuclei **(C)** (black arrows) in the granular cell layer of the OB from AdmHip-enhanced green fluorescent protein (eGFP)-treated mice. The white arrows and arrowheads **(A, B)** indicate the colocalization and the absence of colocalization of the markers, respectively. **(D–F):** In AdmHip-eGFP (Hip) compared with Ad-eGFP (Ctrl), the percentage of BrdU$^+$ cells expressing NeuN (50% ± 3% [total counted cells, n = 1,440] and 54% ± 3% [n = 758], respectively) **(D)** or GFAP (17% ± 2% [n = 281] and 14% ± 1% [n = 171], respectively) **(E)** and the number of TUNEL$^+$ cells (5.9 ± 1.4 [n = 94] and 5.2 ± 1.3 per section [n = 42], respectively) **(F)** were not significantly modified ($p > .05$). Data are the means ± SEM from three to five mice per group. Scale bars = 100 μm **(A, B)** and 50 μm **(C)**. Abbreviations: BrdU, bromodeoxyuridine; Ctrl, control; GFAP, glial fibrillary acidic protein; Hip, Hedgehog interacting protein; NeuN, neuronal nuclei; TUNEL, terminal deoxynucleotidyl transferase dUTP nick-end labeling.

ratio of the number of BrdU$^+$/NeuN$^+$ or BrdU$^+$/GFAP$^+$ cells over the total number of BrdU$^+$ cells was unchanged, indicating that newly generated cells were not influenced preferentially toward a glial or a neuronal phenotype (Fig. 3A, 3B, 3D, 3E). Similar experiments using NG2 as a marker of the oligodendroglial lineage also led to the conclusion that orientation toward this lineage was absent (data not shown). To determine whether BrdU$^+$ cells newly incorporated into the OB have an increased capacity to survive, TUNEL analysis was performed, and no significant difference in the number of apoptotic cells was found between AdmHip-eGFP- and Ad-eGFP-treated mice (Fig. 3C, 3F). Together, these data indicate that Hip treatment does not alter the fate of BrdU$^+$ cells reaching the OB and, moreover, that the large increase in the density of BrdU$^+$ cells observed in the granular layer is not due to an increase in cell survival within the OB.

Neutralizing Shh Monoclonal Antibody 5E1 Mimics Hip Effects in the SVZ and OB In Vivo

The effects described so far may reflect a proper activity of Hip itself, potentially independent of Shh pathway. Thus, to directly block Shh activity in the SVZ, we injected hybridoma cells secreting either the specific neutralizing monoclonal ShhN antibody (5E1) or its control isotype (9E10) [32] into the LV of adult mice (supplemental online Fig. 3). Before the graft, the cells were prestained with the lipidic fluorescent tracer PKH26 to visualize their localization in the brain. Between day 1 and day

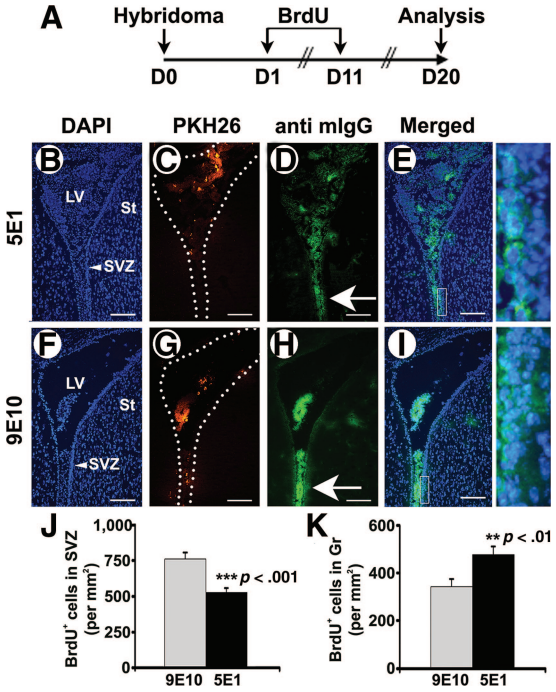

Figure 4. Neutralizing Sonic Hedgehog monoclonal antibody 5E1 mimics the effects of Hedgehog interacting protein in the SVZ and olfactory bulb (OB) in vivo. **(A):** Experimental protocol. **(B–I):** Coronal brain sections from 5E1 **(B–E)** or 9E10 control isotype **(F–I)** hybridoma cell-injected mice analyzed at the level of the LV and SVZ as indicated by DAPI fluorescence **(B, F)**. Prelabeled hybridoma cells (red in **[C, G]**) and secreted 5E1 (green in **[D]**) or 9E10 (green in **[H]**) were visualized 20 days after the intracerebroventricular injection. The dotted line in **(C, G)** delineates the LV wall. The white arrows **(D, H)** indicate 5E1 and 9E10 antibodies in the LV wall. **(E, I):** Correspond to the merge of **(B)** plus **(D)** and **(F)** plus **(H)**, respectively. **(J, K):** In 5E1- compared with 9E10-injected mice, the number of $BrdU^+$ nuclei was decreased in the SVZ (526 ± 30 [total counted cells, $n = 756$] and 761 ± 46 cells per mm^2 [$n = 1,400$], respectively) **(J)** and increased in the Gr of the OB (478 ± 36 [$n = 14,525$] and 9E10, 343 ± 34 cells per mm^2 [$n = 9,917$], respectively) **(K)**. Values are the means ± SEM of six animals per group. **, $p < .01$; ***, $p < .001$. Scale bars = 200 μm. Abbreviations: BrdU, bromodeoxyuridine; D, day; DAPI, 4,6-diamidino-2-phenylindole; Gr, granular cell layer; LV, lateral ventricle; St, striatum; SVZ, subventricular zone.

11 following the graft, the animals received i.p. injections of BrdU, and brain sections were analyzed on day 20 to use the same experimental paradigm as AdmHip-eGFP experiments (Fig. 4A). At the level of the LV, we first observed a red fluorescence, reflecting the presence of the injected cells associated mainly with the ChPl (Fig. 4B, 4C, 4F, 4G). Using anti-mouse IgG immunofluorescence, we then identified the presence of the monoclonal antibodies 5E1 and 9E10 in the ventricular space, the wall of the LV, and also the SVZ, indicating that both antibodies have been secreted and have diffused into the adjacent parenchyma (Fig. 4D, 4E, 4H, 4I) and that 5E1 can interact with the ShhN present in this area. Finally, quantification of $BrdU^+$ cells revealed a 31% decrease ($p < .001$) in the SVZ and a 39% increase ($p < .01$) in the granular cell layer of the OB (Fig. 4J, 4K) of 5E1-treated mice, indicating that direct blocking of Shh mimics the effects induced by Hip overexpression.

Overexpression of Shh In Vivo in the SVZ Induces Effects Opposite Those Mediated by the Blocking of Shh Activity

Then, we investigated the effects induced on migrating neuroblasts by a long-lasting overexpression of Shh in the SVZ in a gain-of-function approach. For this purpose, adult mice were injected with an adenoviral vector bearing the gene encoding Shh (AdhuShh-eGFP) [21] or the corresponding control (Ad-eGFP) into the right LV and allowed to survive 26 days with a daily i.p. injection of BrdU between day 4 and day 18 to reproduce the experimental protocol used with AdmHip-eGFP (Fig. 5A). Upon AdhuShh-eGFP treatment, the mean density of $BrdU^+$ nuclei was significantly increased by 26% ($p < .001$) in the SVZ and decreased by 37% ($p < .01$) in the granular layer of the OB (Fig. 5B, 5C). Thus, the effects induced by overexpression of Shh or blocking of its activity in the SVZ are coherent and result in modulating in the opposite direction the number of $BrdU^+$ cells in the SVZ and in the granular cell layer of the OB. The estimation of the total number of $BrdU^+$ cells in the whole SVZ-RMS-OB system (as described above) led to values corresponding to 104,730 ± 9,241 cells in AdhuShh-eGFP-treated mice versus 125,135 ± 12,364 cells in Ad-eGFP-treated mice ($p > .05$), indicating that, in our model, the increase in $BrdU^+$ nuclei number observed in the SVZ of AdhuShh-eGFP-treated mice (Fig. 5B) does not likely result from a proliferation/survival effect of Shh on adult neural precursors (Fig. 5D). Moreover, an effect of Shh on cell cycle duration or self-renewal of quiescent stem- or transit-amplifying cells in the SVZ is unlikely, since this would imply an increase in $BrdU^+$ cell densities in both the SVZ and OB. However, a modulation by Shh of the migratory properties of newly generated cells on their way toward the OB may account for the effects observed so far in both the SVZ and the OB.

In Vitro Shh Displays a Chemoattractive Activity Mediated by Smo on Migrating Neuroblasts

To investigate whether Shh modulates the migration of neuroblasts newly generated in the SVZ, we performed coculture experiments in collagen matrices using the anterior portion of the SVZ of P6 animals and COS cells transiently overexpressing Shh or not (Fig. 6A–6F; supplemental online Fig. 4). In these experiments the cells from the SVZ explants facing the Shh-transfected COS cells (proximal quadrant) received a high concentration of Shh. In SVZ explants cocultured for 36 hours with control COS cells, cells migrating out of the explants were symmetrically distributed around their circumference (Fig. 6A; supplemental online Fig. 5A). In the presence of Shh-transfected COS cells, cell migration was asymmetric, with more cells migrating into the proximal quadrant (Fig. 6C; supplemental online Fig. 5B). Tuj1 immunolabeling confirmed the neuronal nature of migrating cells in each condition and was used to quantify the proximal/distal ratio of cells migrating out of the SVZ explant (Fig. 6G, 6H). This ratio was significantly higher in the presence of Shh activity than in the control condition (Fig. 6H). When Cur61414 (5 μM), a specific and potent Smo antagonist [33, 34], was added to the collagen matrix and the culture medium, we observed again a symmetric migration (Fig. 6E; supplemental online Fig. 5C). Nevertheless, although the proximal/distal ratio of cells migrating out of the SVZ reached a value significantly different from that obtained in the SVZ-Shh conditions, it was not significantly different from the SVZ-mock condition (Fig. 6H). Furthermore, even though more migrating cells were observed in the proximal quadrant in the presence of Shh, the quantification of the migration distance of neuroblasts in the proximal and distal quadrants revealed no difference compared with control (Fig. 6I). Together, these data demonstrate that Shh can function in vitro in a Smo-dependent manner as a chemoattractant for neuronal progenitors migrating out of SVZ explants, but does not modulate the neuroblast motility. In vivo, ShhN being present in the SVZ itself, it may attract and thus restrain exit of the neuroblasts outside the SVZ,

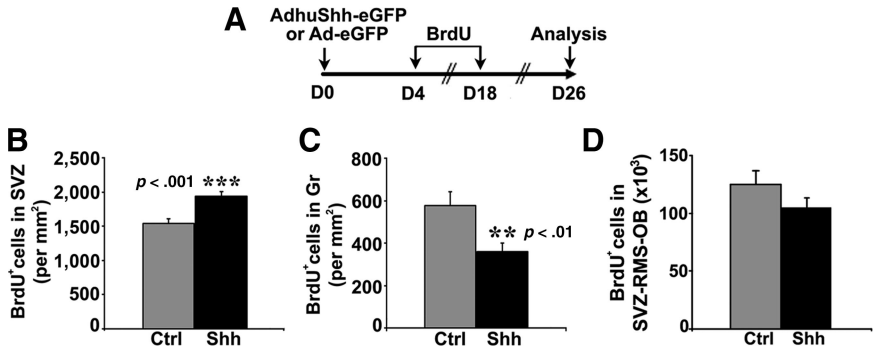

Figure 5. Overexpression of Shh in vivo in the SVZ induces effects opposite those mediated by the blocking of Shh activity. **(A):** Scheme of experimental protocol. **(B, C):** In AdhuShh-eGFP (Shh)- compared with Ad-eGFP (Ctrl)-treated mice, the number of $BrdU^+$ nuclei was increased in the SVZ (1,940 ± 63 [total counted cells, $n = 4{,}755$] and 1,539 ± 70 cells per mm^2 [$n = 3{,}773$], respectively) **(B)** and decreased in the Gr (361 ± 39 [$n = 8{,}239$] and 577 ± 66 cells per mm^2 [$n = 11{,}432$], respectively) **(C)**. **(D):** The total number of $BrdU^+$ cells in the whole SVZ-RMS-OB system was not significantly different in Shh- compared with Ctrl-treated mice (104,730 ± 9,241 and 125,135 ± 12,364 cells, respectively; $p > .05$). The volumes (mm^3) of the structures determined for Shh- and Ctrl-treated mice were as follows: 0.151 ± 0.010 and 0.164 ± 0.002 (SVZ); 0.268 ± 0.027 and 0.208 ± 0.009 (RMS); and 2.387 ± 0.233 and 2.480 ± 0.073 (OB), respectively. Data are the means ± SEM from five or six mice per group. **, $p < .01$; ***, $p < .001$. Abbreviations: BrdU, bromodeoxyuridine; Ctrl, control; D, day; Gr, granular cell layer; eGFP, enhanced green fluorescent protein; OB, olfactory bulb; RMS, rostral migratory stream; Shh, Sonic Hedgehog; SVZ, subventricular zone.

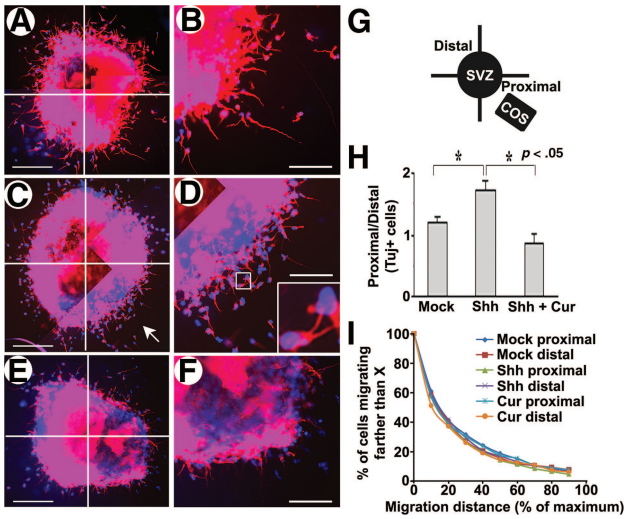

Figure 6. Shh acts as a chemoattractant for migrating neuroblasts in vitro. **(A–F):** Epifluorescence microscopy analysis of cell migration on SVZ explants cocultured with COS(mock) **(A, B)** and COS(Shh) cells in the absence **(C, D)** or presence **(E, F)** of 5 μM Cur. Cell nuclei (4,6-diamidino-2-phenylindole; blue) and neuroblasts (Tuj1, red) are shown. **(B, D, F):** Enlargements of the proximal quadrants in **(A)**, **(C)**, and **(E)**, respectively. **(G):** Cell aggregates are located in the bottom right quadrant. The arrow in **(C)** shows the higher number of cells migrating in the quadrant containing the COS(Shh) cells compared with the opposite quadrant. **(H, I):** Proximal/distal ratios of the number of migrating neuroblasts (SVZ-Shh, 1.72 ± 0.18; $n = 41$ explants; total number of counted cells, 3,065; SVZ-mock, 1.20 ± 0.11; $n = 45$ explants; total number of counted cells, 2,942; SVZ-Shh + Cur, 0.88 ± 0.14; $n = 13$ explants; total number of counted cells, 776) **(H)** and their migration distance (in percentage of the maximal distance covered by cells in each quadrant) **(I)** in the above conditions. *, $p < .05$. Data are means ± SEM. Scale bars = 100 μm **(A, C, E)** and 50 μm **(B, D, F)**. Abbreviations: Cur, Cur61414; Shh, Sonic Hedgehog; SVZ, subventricular zone; Tuj1, neuron-specific class III beta-tubulin.

which would be in agreement with the effects induced by either the blocking or the overexpression of Shh in the SVZ.

Ectopic Shh Overexpression Causes the Migrating Neuroblasts to Deviate from Their Normal Pathway

To determine whether Shh displays a chemoattractant activity in vivo on the migrating neuroblasts, we ectopically grafted control or Shh-expressing QT6 cells prestained with PKH26 to overexpress ShhN locally in the dorsal telencephalon, above the RMS in an area void of progenitor cells. Four days later, Shh protein was detected close to the RMS in mice grafted with Shh-expressing cells but not in animals receiving the control QT6 cells (supplemental online Fig. 6A, 6B; data not shown). In addition, we observed a thickening of the RMS, as well as $PSA\text{-}NCAM^+$ migrating neuroblasts entering the area located between the graft and the RMS, often as chains (Fig. 7C, 7D). Such observations were never done in the control mice (Fig. 7A, 7B). Quantification of the number of neuroblasts deviating from the pathway regularly used by the migrating cells (Fig. 7E) indicated a fourfold increase in animals displaying the ectopic expression of Shh, suggesting that in vivo Shh has the capacity to attract the migrating neuroblasts away from the RMS. We have also quantified the total number of $BrdU^+$ cells in sagittal sections containing the grafted cells and the greatest extent of the RMS in QT6-Shh-treated animals compared with the control QT6-treated mice (supplemental online Fig. 7A). QT6-Shh-grafted mice had 422 ± 11 $BrdU^+$ cells per slice versus 422 ± 78 in the controls (supplemental online Fig. 7B), indicating that the total number of $BrdU^+$ cells counted in the RMS was not significantly different in QT6-Shh-treated mice compared with QT6-treated mice. Consequently, the thickening of the RMS observed in the presence of QT6-Shh is likely related to the accumulation of cells and not to cell proliferation/survival. Taken together, these data strongly support a contribution of Shh in vivo in the tangential migration of neuroblasts from the SVZ to the OB, consistent with its capacity to retain migrating neuroblasts in the SVZ.

DISCUSSION

The tangential migration process that leads the neuroblasts newly generated in the SVZ to travel along the RMS toward the OB is regulated by molecules that repel the neuroblasts away from the SVZ and regulate cell motility and cell chain formation throughout the RMS. Other factors derived from the OB attract the neuroblasts [3]. We are now providing new observations suggesting that the morphogen Shh present in the SVZ and CSF is a molecular cue responsible for the control of migrating neuroblasts exiting the SVZ and thus reaching the OB.

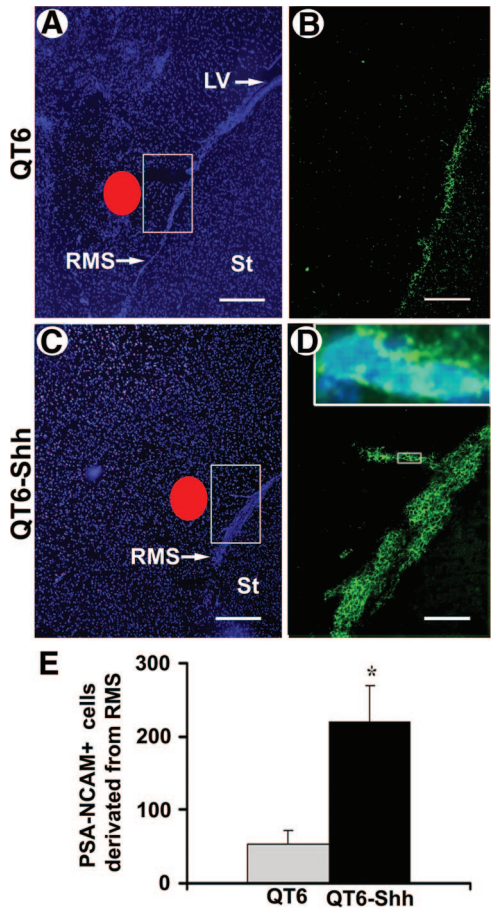

Figure 7. Ectopic expression of Shh diverts migrating neuroblasts from their regular pathway. **(A–D):** Immunofluorescence of sagittal brain sections from mice grafted above the RMS with mock- (QT6; red circle in **[A]**) or Shh- (QT6-Shh; red circle in **[C]**) stable cell lines. Cell nuclei (4,6-diamidino-2-phenylindole; blue in **[A, C]**) and migrating neuroblasts (PSA-NCAM, green in **[B, D]**) are shown. **(B)** and **(D):** Correspond to PSA-NCAM immunofluorescence observed in the boxed regions in **(A)** and **(C)**, respectively. Compared with controls **(A, B)**, the RMS was thicker **(C)**, and neuroblasts migrated toward the graft (**[D]**, boxed area and inset) in the presence of QT6-Shh cells. **(E):** Quantification of neuroblasts diverted from the RMS by counting PSA-NCAM$^+$ cells located outside the normal migratory pathway (QT6-Shh, 220 ± 49 cells, total counted cells, $n = 880$; QT6, 53 ± 19; $n = 266$). *, $p < .05$. Values are means ± SEM from four animals. Scale bars, 400 μm **(A, C)** and 100 μm **(B, D)**. Abbreviations: LV, lateral ventricle; PSA-NCAM, poly-sialated neural cell adhesion molecule; RMS, rostral migratory stream; Shh, Sonic Hedgehog; St, striatum.

First, our work shows that the ShhN protein is present in striatal tissue strips containing the SVZ and in the CSF of adult mice, in agreement with previous data reporting the presence of Shh transcripts within SVZ cells of adult mice [26] and with our previous work showing ShhN expression in SVZ extracts of adult rats [14]. Then, we demonstrated that Ptc and Smo transcripts are present in the SVZ and RMS of adult mice, and using the Ptc$^{+/-}$ *LacZ* reporter mouse line, we showed that Ptc is expressed on PSA-NCAM$^+$ migrating neuroblasts, indicating that these cells can respond to Shh. To further analyze the potential role of Shh present in the SVZ and CSF on migrating neuroblasts in vivo, we directly addressed the effects of either the prolonged overexpression of Shh in the SVZ or the direct blockade of its activity with Hip or blocking monoclonal antibodies, two well-characterized Shh-specific antagonists. These gain- and loss-of-function experiments led to concordant results in the SVZ and the OB. Blocking Shh activity in vivo in the SVZ induced a significant decrease in the number of BrdU$^+$ cells in the SVZ and, in parallel, an increase in the OB without modification of the survival or phenotype of cells reaching the OB. Conversely, overexpressing Shh in the SVZ led to an increase in the number of BrdU$^+$ cells in the SVZ and a decrease in the OB. Furthermore, we observed that the number but not the motility of neuroblasts migrating out of SVZ explants increased when these explants were cocultured with Shh-expressing cells, which demonstrates the chemoattractive activity of the morphogen in vitro. Finally, Shh displayed a chemoattractive activity on the neuroblasts in vivo, since Shh-expressing cells grafted above the RMS of adult mice induced the migrating neuroblasts to deviate out of their normal way, the RMS. As a whole, these results are consistent with the ability of Shh to modulate neuroblast exit out of the SVZ, likely by attracting these cells (thus restraining their progression) within the niche.

The presence of Ptc and Smo in both the SVZ and along the RMS of adult mice and the inhibition induced by a Smo antagonist on Shh chemoattractive effects in SVZ explants indicate that Shh activity on SVZ-derived neuroblasts is likely mediated by its classic Ptc/Smo receptor tandem. Nevertheless, the absence of Gli1 expression previously reported in these cells [22, 25] suggests that this response may be mediated through other members of the Gli family. In agreement with this hypothesis, the attenuation of the Gli3 repressor, an activity occurring in the absence of Gli1 expression, has been described during the dorsoventral patterning of the telencephalon [35] and midbrain [36]. Alternatively, this response may occur in a Gli-independent manner and also not involve gene transcription, as was recently proposed for Shh-induced cell motility, migration, axonal growth, and extension of spinal and retinal neurons [8, 13, 37, 38] or for the modification of the electrophysiological response of mature neurons triggered within a few minutes after exposure to Shh [18, 19].

The mechanism through which Shh is acting as a chemoattractant has been addressed in the neural tube. Shh was shown to control dispersion of neural crest cells from the dorsal neural tube by inhibiting their integrin-mediated adhesiveness [39] and also to modulate the adhesive and migratory capacities of neuroepithelial cells through inactivation of surface β1-integrins combined with an increase in N-cadherin-mediated cell adhesion [40]. Since β1 integrins expressed by neuroblasts were recently demonstrated to control the formation of cell chains in the adult RMS [5], it would be interesting to analyze whether Shh and integrin pathways are still able to interact in the adult SVZ. Shh transcription is reduced in an animal model of Parkinson's disease [18], indicating that dopamine depletion in the basal ganglia may alter Shh signaling. Whether such depletion also affects Shh levels in the SVZ and whether other proteins shown to interact with Shh [11, 12, 41] also regulate Shh-mediated retention effects described here should also be further investigated.

Our gain- and loss-of-function experiments modulate the number of SVZ-derived cells reaching the OB. Moreover, they support a role of Shh in regulating the neuroblast migration through the SVZ-RMS, but likely not in modulating the proliferation/survival of SVZ-derived precursors. Previous reports using either Smo removal during embryo and postnatal life [22–24] or the blocking of its activity with a systemic injection of the Smo antagonist cyclopamine [26] had revealed an increase in cell death in the SVZ and a decrease in cell proliferation in both the SVZ and the OB, respectively. Together, these data suggest that, in the SVZ, Smo may mediate its proliferation/survival activity independently of Shh signaling, through a yet-unknown endogenous ligand [42, 43]. Smo may also trans-

duce Shh chemoattractive activity through its classic association with Ptc. This hypothesis would also be in agreement with previous data reporting that an acute injection of recombinant ShhN into the LV does not increase cell proliferation in the SVZ in vivo [21] and that Shh is unable to support neurosphere expansion in the absence of EGF in vitro [26]. As a whole, these observations suggest the role of Hh signaling components in the SVZ-OB system is likely much more complex than was initially thought and moreover not systematically conserved during development. In agreement with this observation, Smo removal in embryonic day 12.5 mice has been associated with a failure in neuroblast migration, presumably via an indirect effect that may result from a nonautonomous signaling possibly caused by a reduction of Slit1 ligand in the neuroblasts [22], whereas in adulthood, Shh is a chemoattractant factor involved in an autonomous manner in the regulation of neuroblast migration.

Recently, the close association of olfactory memory with the level of ongoing neurogenesis in the SVZ-OB system was shown [44]. By modulating the number of new neurons migrating in this system, Shh could add another degree of plasticity in this process. In addition, the unique capacity of this system for continuously providing new cells is of major importance in view of brain repair approaches. In this respect, the pharmacological modulation of Shh activity on the neuroblasts might be of particular interest and lead to a better understanding of the pathologies where the number and the capacity of migration of neuroblasts are reduced, as recently shown in animal models of Parkinson's disease [45]. Future studies should also reveal whether Shh-attractive activity intervenes in the inappropriate cell migration occurring in metastasis of brain tumors associated with dysregulation of the Hh pathway [33, 46].

CONCLUSION

In summary, we show that ShhN is present in the SVZ stem cell niche and that its receptor, Ptc, is expressed on migrating neuroblasts. Overexpression and blocking of Shh in the SVZ induce a modulation of the number of proliferating cells in the SVZ and the OB in the opposite direction, which agrees with the chemoattractive activity exerted by Shh on migrating neuroblasts in vitro and in vivo. Together, these observations provide evidence that the exit of migrating neuroblasts out of the SVZ results from a equilibrium between chemoattractive and chemorepulsive activities.

ACKNOWLEDGMENTS

We thank A. Mann and A. Schoenfelder (Centre National de la Recherche Scientifique, Unité Mixte de Recherche 7081, Illkirch, France) for the synthesis of Cur61414, V. Zuliani and the Production Service Unit of Genethon for large-scale production of adenoviral vectors (http://www.genethon.fr), A.P. McMahon (Harvard, Cambridge, MA) for Hip vector, D. Duprez (Université Pierre et Marie Curie, France) for providing QT6-Shh cells, E.T. Stoeckli (University of Zurich, Switzerland) for the hybridoma cell lines, and H. Faure for technical advice. E.A. is the recipient of a doctoral fellowship from the Ministère de la Recherche. This work was supported by grants from Association Française contre les Myopathies, Association pour la Recherche contre le Cancer, la Ligue contre le Cancer, Association pour la Recherche sur la Sclérose en Plaque, Institut National du Cancer, and the French Agence Nationale de la Recherche (number 07-physio-010-04). K.T.N.-B.-C. is currently affiliated with Institut National de la Santé et de la Recherche Médicale, Institut de la Vision, Paris, France.

DISCLOSURE OF POTENTIAL CONFLICTS OF INTEREST

The authors indicate no potential conflicts of interest.

REFERENCES

1 Zhao C, Deng W, Gage FH. Mechanisms and functional implications of adult neurogenesis. Cell 2008;132:645–660.
2 Doetsch F, Garcia-Verdugo JM, Alvarez-Buylla A. Cellular composition and three-dimensional organization of the subventricular germinal zone in the adult mammalian brain. J Neurosci 1997;17:5046–5061.
3 Lledo PM, Alonso M, Grubb MS. Adult neurogenesis and functional plasticity in neuronal circuits. Nat Rev Neurosci 2006;7:179–193.
4 Sawamoto K, Wichterle H, Gonzalez-Perez O et al. New neurons follow the flow of cerebrospinal fluid in the adult brain. Science 2006;311:629–632.
5 Belvindrah R, Hankel S, Walker J et al. Beta1 integrins control the formation of cell chains in the adult rostral migratory stream. J Neurosci 2007;27:2704–2717.
6 Fu M, Lui VC, Sham MH et al. Sonic hedgehog regulates the proliferation, differentiation, and migration of enteric neural crest cells in gut. J Cell Biol 2004;166:673–684.
7 Gering M, Patient R. Hedgehog signaling is required for adult blood stem cell formation in zebrafish embryos. Dev Cell 2005;8:389–400.
8 Charron F, Stein E, Jeong J et al. The morphogen sonic hedgehog is an axonal chemoattractant that collaborates with netrin-1 in midline axon guidance. Cell 2003;113:11–23.
9 Okada A, Charron F, Morin S et al. Boc is a receptor for sonic hedgehog in the guidance of commissural axons. Nature 2006;444:369–373.
10 Bourikas D, Pekarik V, Baeriswyl T et al. Sonic hedgehog guides commissural axons along the longitudinal axis of the spinal cord. Nat Neurosci 2005;8:297–304.
11 Fuccillo M, Joyner AL, Fishell G. Morphogen to mitogen: The multiple roles of hedgehog signalling in vertebrate neural development. Nat Rev Neurosci 2006;7:772–783.
12 Ingham PW, Placzek M. Orchestrating ontogenesis: Variations on a theme by sonic hedgehog. Nat Rev Genet 2006;7:841–850.
13 Riobo NA, Manning DR. Pathways of signal transduction employed by vertebrate Hedgehogs. Biochem J 2007;403:369–379.
14 Charytoniuk D, Traiffort E, Hantraye P et al. Intrastriatal sonic hedgehog injection increases Patched transcript levels in the adult rat subventricular zone. Eur J Neurosci 2002;16:2351–2357.
15 Coulombe J, Traiffort E, Loulier K et al. Hedgehog interacting protein in the mature brain: Membrane-associated and soluble forms. Mol Cell Neurosci 2004;25:323–333.
16 Traiffort E, Charytoniuk D, Watroba L et al. Discrete localizations of hedgehog signalling components in the developing and adult rat nervous system. Eur J Neuroscience 1999;11:3199–3214.
17 Traiffort E, Moya KL, Faure H et al. High expression and anterograde axonal transport of aminoterminal sonic hedgehog in the adult hamster brain. Eur J Neurosci 2001;14:839–850.
18 Bezard E, Baufreton J, Owens G et al. Sonic hedgehog is a neuromodulator in the adult subthalamic nucleus. FASEB J 2003;17:2337–2338.
19 Pascual O, Traiffort E, Baker DP et al. Sonic hedgehog signalling in neurons of adult ventrolateral nucleus tractus solitarius. Eur J Neurosci 2005;22:389–396.
20 Lai K, Kaspar BK, Gage FH et al. Sonic hedgehog regulates adult neural progenitor proliferation in vitro and in vivo. Nat Neurosci 2003;6:21–27.
21 Loulier K, Ruat M, Traiffort E. Increase of proliferating oligodendroglial progenitors in the adult mouse brain upon Sonic hedgehog delivery in the lateral ventricle. J Neurochem 2006;98:530–542.
22 Balordi F, Fishell G. Hedgehog signaling in the subventricular zone is required for both the maintenance of stem cells and the migration of newborn neurons. J Neurosci 2007;27:5936–5947.
23 Balordi F, Fishell G. Mosaic removal of hedgehog signaling in the adult SVZ reveals that the residual wild-type stem cells have a limited capacity for self-renewal. J Neurosci 2007;27:14248–14259.
24 Machold R, Hayashi S, Rutlin M et al. Sonic hedgehog is required for progenitor cell maintenance in telencephalic stem cell niches. Neuron 2003;39:937–950.

25 Ahn S, Joyner AL. In vivo analysis of quiescent adult neural stem cells responding to Sonic hedgehog. Nature 2005;437:894–897.
26 Palma V, Lim DA, Dahmane N et al. Sonic hedgehog controls stem cell behavior in the postnatal and adult brain. Development 2005;132:335–344.
27 Goodrich LV, Milenkovic L, Higgins KM et al. Altered neural cell fates and medulloblastoma in mouse patched mutants. Science 1997;277:1109–1113.
28 Petreanu L, Alvarez-Buylla A. Maturation and death of adult-born olfactory bulb granule neurons: Role of olfaction. J Neurosci 2002;22:6106–6113.
29 Nguyen-Ba-Charvet KT, Picard-Riera N, Tessier-Lavigne M et al. Multiple roles for slits in the control of cell migration in the rostral migratory stream. J Neurosci 2004;24:1497–1506.
30 Chazal G, Durbec P, Jankovski A et al. Consequences of neural cell adhesion molecule deficiency on cell migration in the rostral migratory stream of the mouse. J Neurosci 2000;20:1446–1457.
31 Hack MA, Saghatelyan A, de Chevigny A et al. Neuronal fate determinants of adult olfactory bulb neurogenesis. Nat Neurosci 2005;8:865–872.
32 Ericson J, Morton S, Kawakami A et al. Two critical periods of Sonic Hedgehog signaling required for the specification of motor neuron identity. Cell 1996;87:661–673.
33 Borzillo GV, Lippa B. The Hedgehog signaling pathway as a target for anticancer drug discovery. Curr Top Med Chem 2005;5:147–157.
34 Masdeu C, Faure H, Coulombe J et al. Identification and characterization of Hedgehog modulator properties after functional coupling of Smoothened to G15. Biochem Biophys Res Commun 2006;349:471–479.
35 Rallu M, Machold R, Gaiano N et al. Dorsoventral patterning is established in the telencephalon of mutants lacking both Gli3 and Hedgehog signaling. Development 2002;129:4963–4974.
36 Blaess S, Corrales JD, Joyner AL. Sonic hedgehog regulates Gli activator and repressor functions with spatial and temporal precision in the mid/hindbrain region. Development 2006;133:1799–1809.
37 Bijlsma MF, Borensztajn KS, Roelink H et al. Sonic hedgehog induces transcription-independent cytoskeletal rearrangement and migration regulated by arachidonate metabolites. Cell Signal 2007;19:2596–2604.
38 Kolpak A, Zhang J, Bao ZZ. Sonic hedgehog has a dual effect on the growth of retinal ganglion axons depending on its concentration. J Neurosci 2005;25:3432–3441.
39 Testaz S, Jarov A, Williams KP et al. Sonic hedgehog restricts adhesion and migration of neural crest cells independently of the Patched-Smoothened-Gli signaling pathway. Proc Natl Acad Sci U S A 2001;98:12521–12526.
40 Jarov A, Williams KP, Ling LE et al. A dual role for Sonic hedgehog in regulating adhesion and differentiation of neuroepithelial cells. Dev Biol 2003;261:520–536.
41 Tenzen T, Allen BL, Cole F et al. The cell surface membrane proteins Cdo and Boc are components and targets of the Hedgehog signaling pathway and feedback network in mice. Dev Cell 2006;10:647–656.
42 Bijlsma MF, Spek CA, Zivkovic D et al. Repression of smoothened by patched-dependent (pro-)vitamin D3 secretion. PLoS Biol 2006;4:e232.
43 Corcoran RB, Scott MP. Oxysterols stimulate Sonic hedgehog signal transduction and proliferation of medulloblastoma cells. Proc Natl Acad Sci U S A 2006;103:8408–8413.
44 Romero-Grimaldi C, Gheusi G, Lledo PM et al. Chronic inhibition of nitric oxide synthesis enhances both subventricular zone neurogenesis and olfactory learning in adult mice. Eur J Neurosci 2006;24:2461–2470.
45 Freundlieb N, Francois C, Tande D et al. Dopaminergic substantia nigra neurons project topographically organized to the subventricular zone and stimulate precursor cell proliferation in aged primates. J Neurosci 2006;26:2321–2325.
46 Beachy PA, Karhadkar SS, Berman DM. Tissue repair and stem cell renewal in carcinogenesis. Nature 2004;432:324–331.

See www.StemCells.com for supplemental material available online.